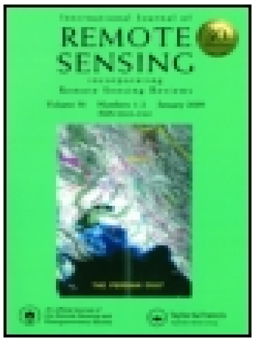

International Journal of Remote Sensing

ISSN: 0143-1161 (Print) 1366-5901 (Online) Journal homepage: http://www.tandfonline.com/loi/tres20

Comprehensive comparison of daily IMERG and GSMaP satellite precipitation products in Ardabil Province, Iran

Farnoosh Aslami, Ardavan Ghorbani, Behrooz Sobhani & Abazar Esmali

INTERNATIONAL JOURNAL OF REMOTE SENSING
https://doi.org/10.1080/01431161.2018.1539274

Taylor & Francis
Taylor & Francis Group

Check for updates

Comprehensive comparison of daily IMERG and GSMaP satellite precipitation products in Ardabil Province, Iran

Farnoosh Aslami[a], Ardavan Ghorbani[b], Behrooz Sobhani[a] and Abazar Esmali[b]

[a]Dept. of Natural Geography, Faculty of Humanities, University of Mohaghegh Ardabili, Ardabil, Iran; [b]Dept. of Natural Resources, Faculty of Agriculture and Natural Resources, University of Mohaghegh Ardabili, Ardabil, Iran

ABSTRACT

The measurement of precipitation is essential for most environmental studies such as drought monitoring, watershed operations, water hazard management, etc. Development of satellite products has improved their applicability in environmental modelling and could proffer an alternative to gauge-based precipitation data, particularly in areas where there is no sufficient number of gauges or poor gauge distribution but they should be evaluated in different areas using ground-based data as references. In the present study, daily Integrated Multi-satellitE Retrievals for the Global Precipitation Measurement (GPM- IMERG- Final (Version 5)) and Global Satellite Mapping of Precipitation-Moving Vector with Kalman filter (GSMaP-MVK (Version 7)) precipitation products were evaluated in comparison with gauges observations in Ardabil province, north-west of Iran, from 1 January 2016 to 21 October 2017. Several statistical indices including linear correlation coefficient, Bias (B), Multiplicative Bias (B_m), Relative Bias (B_r), Mean Absolute Error (MAE), Root Mean Square Error (RMSE), Probability of Detection (POD), False Alarm Ratio (FAR) and Critical Success Index (CSI) were used for evaluation. The results showed that the correlation between GSMaP estimates and gauge observations is higher than that of IMERG (0.42 and 0.33, respectively). On the other hand, GSMaP tends to overestimate precipitation substantially, while IMERG is involved in both under and overestimation slightly. Although these products could not show very high accuracy in precipitation estimation, the estimated precipitation values by IMERG were relatively closer to gauge records and can be used as a replacement for gauge observation in the study area where there is lack of weather stations.

ARTICLE HISTORY
Received 27 March 2018
Accepted 20 August 2018

1. Introduction

The measurement of precipitation is essential for most environmental studies such as drought monitoring (Bijaber et al. 2018), watershed operations (Kane et al. 2000), water hazard management (Hermance and Sulieman 2018), etc. Moreover, precipitation is one of the most important inputs for hydrological related models; therefore, an accurate

CONTACT Ardavan Ghorbani ardavanica@yahoo.com Faculty of Agricultural Technology and Natural Resources, University of Mohaghegh Ardabili, Ardabil, Iran

estimate of precipitation is a great concern (Kurtzman, Navon, and Morin 2009; Li, Zhang, and Xu 2012). Interpolation of gauges data can be used for conventional estimates of real precipitation (Frei and Schar 1998; Luo, Xu, and Shi 2011; Zeinivand 2015). There are various interpolation methods (Guillermo, Tabios, and Salas 1985), including Thiessen polygons (Thiessen 1911), inverse distance weighting (IDW) (Watson and Philips 1985) and Kriging (Griffith 1988; Bailey and Gatrell 1995) which are widely applied for estimation of precipitation (Keblouti, Ouerdachi, and Boutaghane 2012). Sometimes, application of these methods could yield incorrect results due to topographical variation in the area and limited available gauge number (Sawunyama and Hughes 2008). Moreover, their results can be affected by the heterogeneity of the random fields (Ball and Luk 1998). In addition, most interpolation methods tend to produce smooth output, which will affect the extreme value estimations (Skaugen and Andersen 2010). On the other hand, sometimes, it is impossible economically to create much more number of precipitation gauges. Recent development in satellite products has improved their applicability in environmental modelling and could proffer an alternative to gauge-based estimates (Barrett et al. 1988; Sawunyama and Hughes 2008). The main advantage of satellite-derived data is its temporal coverage and spatial variability, which can be applied for successful hydrological analysis (Hossain et al. 2007). Up to this point, several advanced satellite-derived precipitation retrieving products such as Tropical Rainfall Measuring Mission (TRMM) Multi-satellite Precipitation Analysis (TMPA) (Huffman et al. 2007), Precipitation Estimation from Remote Sensed Information Using Artificial Neural Networks-Cloud Classification System (PERSIANN-CCS) (Hong et al. 2007), Climate Prediction Center (CPC) Morphing Technique Product (CMORPH) (Joyce et al. 2004), Global Satellite Mapping of Precipitation (GSMaP) (Okamoto et al. 2005; Kubota et al. 2007), etc., have been generated. The TRMM successor, the Global Precipitation Measurement (GPM) which was initiated by National Aeronautics and Space Administration (NASA) and Japanese Aerospace Exploration Agency (JAXA) on 27 February 2014 from Tanegashima Space Center, Japan (Hou et al. 2014; Huffman, Bolvin, and Nelkin 2015) has provided global precipitation products with higher spatial/temporal resolution. As compared to TRMM, the capability of precipitation detection by GPM Core Observatory is enhanced significantly because it has a greater number of channels in the multi-channel GPM Microwave Imager (GMI) and the first space-borne K_u/K_a-band Dual-Frequency Precipitation Radar (DPR) instruments. The DPR consists of a K_a-band precipitation radar (K_aPR at 35.50 GHz) and a K_u-band precipitation radar (K_uPR at 13.60 GHz) (Skofronick-Jackson et al. 2013). According to Skofronick-Jackson et al. (2013) and Huffman, Bolvin, and Nelkin (2015), the DPR is more sensitive to light precipitation rates and the overlapping of K_a/K_u -bands of the DPR provides more accurate information on particle drop size. In addition, GMI covers a swath of 885 km (in 10.00 GHz to 183.00 GHz frequency ranges). The frequencies used by GMI have been optimized to retrieve precipitation in different severities (heavy, moderate, and light precipitation) and falling snow by calculating the polarization difference at each channel as well as a fully parametric approach using a Byaesian inversion (Kummerow et al. 2015). Since 12 March 2014, NASA has released Integrated Multi-satellitE Retrievals for GPM (IMERG), providing half hourly multi-satellite precipitation product with a $0.10° \times 0.10°$ spatial resolution which is expected to measure light precipitation (less than 0.50 mm h^{-1}) (Skofronick-Jackson et al. 2013). IMERG is designed to inter-calibrate, merge, and interpolate all microwave estimates of the GPM constellation, infrared estimates, gauge observations, and other sensors data (Huffman et al. 2018).

Meanwhile, a precipitation retrieving algorithm was upgraded by JAXA using passive microwave information from GMI and released the newest version of GSMaP (Version 6 and 7) (Okamoto et al. 2005; Kubota et al. 2007; Aonashi et al. 2009; Ushio et al. 2009). Spatial and temporal resolutions of GSMaP are 0.10° × 0.10° and hourly, respectively. Both IMERG and GSMaP are known as GPM-era satellite precipitation products (GSPPs). The GSMaP algorithm consists of the following steps: 1) calculating the precipitation rate from passive microwave sensors; 2) using Morphing technique to propagate precipitation affected area; and 3) refining the estimated data using Kalman filter approach (Aonashi et al. 2009). Moreover, the Japan Meteorological Agency Global Analysis (JMAGANAL) data and Merged Satellite/in situ Global Daily Sea Surface Temperatures (MGDSST) are used for the development of the algorithm as inputs (Chen and Li 2016). A detailed explanation of GSMaP data formats and different sorts of this product can be found in the work of Okamoto et al. (2005).

There are many studies on evaluation of satellite-based precipitation products throughout the world (Chiu, Shin, and Kwaitkowski et al. 2006; Hong et al. 2007; Moazami et al. 2013; Li, Zhang, and Xu 2014; Chen and Li 2016). As for IMERG and GSMaP, Chen and Li (2016) and Ning et al. (2016) evaluated IMERG products in Mainland China on a monthly scale. Ning et al. (2016) used GSMaP in addition to IMERG from April 2014 to November 2015 at daily/monthly resolutions and reported that in terms of statistics, GSMaP was more able to estimate precipitation than IMERG. Moreover, Xu, Shen, and Du (2016) and Tang et al. (2016) used IMERG data for warm seasons in 2014 and 2015 which could not be generalized for other seasons. Sharifi, Steinacker, and Saghafian (2016) compared IMERG with TRMM at daily scale for 4 different regions of Iran and showed that IMERG generally had better performance. Khodadoust Siuki, Saghafian, and Moazami (2017) evaluated IMERG and TRMM hourly data in Khorasan Razavi province, Iran, and showed that IMERG had reasonable agreement with the gauge-based observations. Krishna et al. (2017) compared IMERG with TRMM (TMPA, also known as 3B42) in Western Ghats of India and they reported that the correlation coefficient of IMERG with gauge-based observations was higher. Ning et al. (2017) compared IMERG and GSMaP data in several basins in China, from April 2014 to March 2016. Their results showed that spatial distribution of total bias of both products was different, but the GSMaP data generally had a higher accuracy than the IMERG. Prakash et al. (2016) compared TMPA, IMERG and GSMaP with gauge-based observations in India with a daily scale (June to September 2014). They reported that IMERG's variability is more realistic than TMPA and GSMaP data.

Satellite-derived precipitation products can present spatially steady measurement; however, their efficiency in hydrologic applications changes regionally due to several factors including the algorithms used for retrieving, instrument features, survey time, etc. (Su, Hong, and Lettenmaier 2008; Bitew and Gebremicheal 2011; Saber and Yilmaz 2016; Yoshinoto and Amarnath 2016; Kim et al. 2016; Bajracharya, Shrestha, and Shrestha 2017).

Ardabil province located in north-west of Iran is a mountainous area with limited precipitation gauge stations, particularly at high altitudes; thus, the aim of this study was to compare precipitation gauge data with satellite-derived IMERG-Final (Version 5) (IMERG database 2018) and GSMaP-MVK (Moving Vector with Kalman filter) (Version 7) (GSMaP database 2018) precipitation products in daily scale (from 00:00:00 to 23:59:59) in Ardabil province (the data are mentioned as IMERG and GSMaP for conciseness throughout the paper). It should be noted that the downloaded daily GSMaP data are averaged daily data (mm h^{-1}). To the best of the authors' knowledge, there is no report on evaluation of IMERG and GSMaP dataset in Iran including Ardabil Province.

2. Materials and methods

2.1. *Study area*

Ardabil province with an area of 1.80 million km^2 is located north-west of Iran (Figure 1). The elevation from sea level in the area varies from about 20 m to 4811 m. Two third of the study area has mountainous texture with high altitude differences and the rest part is plain and flat. According to the Ardabil Province Meteorological Organization's statistics, the western part of the area (Mt. Sabalan) has the highest average annual precipitation (between 400 mm and 500 mm); but this amount is reduced in other parts and reaches 350 mm in the south and 210 mm to 240 mm in the north of the province. Moreover, average minimum and maximum temperatures in the study area are 1.50°C and 20.50°C, respectively (Kakeh Mami et al. 2017; Aslami and Ghorbani, 2018).

2.2. *Precipitation data*

Although in the study area, there are no adequate gauges for precipitation measurement, considering the aim of the study, gauge data were used as the reference for

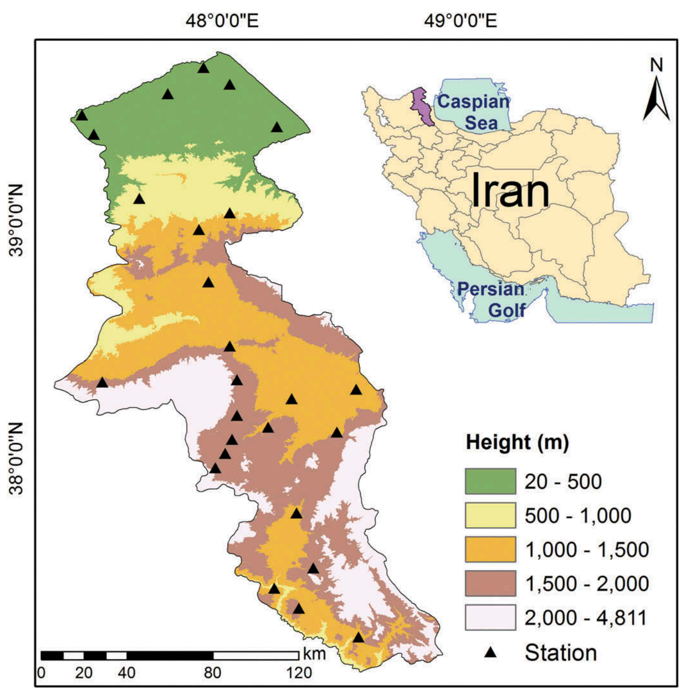

Figure 1. The study area location, digital elevation model (DEM) and gauges locations.

evaluation of satellite-derived precipitation products. According to their spatial distribution and the completeness of the desired data, a total of 27 gauges, including 10 synoptic and 17 precipitation stations were selected. Observed precipitation statistics in daily scale from 1 January 2016 to 21 October 2017 were taken from the Ardabil Province Meteorological Organization. On the other hand, IMERG and GSMaP data were downloaded for the same period and time scales, in '.nc' and '.csv' formats, respectively. As previously described, IMERG data enhanced capabilities to measure light precipitation (less than 0.50 mm h^{-1}) with 0.10° × 0.10° spatial resolution and 30 min temporal resolution (Skofronick-Jackson et al. 2013; Huffman et al. 2014) and the newest versions of GSMaP products use GMI tool of GPM. It should be noted that daily GSMaP data are averaged data (mm h^{-1}); therefore, they should be rescaled by 24 to be converted to mm day^{-1}.

2.3. *Validation*

Nine statistical indices were used to evaluate the performance of satellite-derived data as compared to gauge records. The Bias, B, is the average difference between gauge records and satellite-derived data (Equation (1)). Underestimations are shown with a negative Bias and overestimations resulted in positive ones. Multiplicative Bias (B_m) is defined as the ratio of satellite values and the observed values (gauges) (Equation (2)). B_m values less than one show underestimation and greater than one show overestimation. Relative Bias (B_r) is the systematic bias of satellite-derived precipitation and could be described as similar to the Bias (Equation (3)). Mean Absolute Error (MAE) presents the average magnitude of the error (Equation (4)). Root Mean Square Error (RMSE) is similar to MAE, but gives a greater weight to larger errors by showing the overall error magnitude (Equation (5)). The correlation coefficient (r) presents the degree of agreement between two data sets, ranging from – 1 to +1 and indicating perfect negative and positive fit, respectively (Equation (6)). r will be close to 0 if there is no linear correlation or a weak linear correlation (Moazami et al. 2013).

$$B = \frac{\sum_{i=1}^{N}\left(P_{S,i} - P_{O,i}\right)}{N} \tag{1}$$

$$B_m = \frac{\sum_{i=1}^{N} P_{S,i}}{\sum_{i=1}^{N} P_{O,i}} \tag{2}$$

$$B_r(\%) = \frac{\sum_{i=1}^{N}\left(P_{S,i} - P_{O,i}\right)}{\sum_{i=1}^{N} P_{O,i}} \; 100 \tag{3}$$

$$\text{MAE} = \frac{\sum_{i=1}^{N}\left|P_{S,i} - P_{O,i}\right|}{N} \tag{4}$$

$$\text{RMSE} = \left[\frac{\sum_{i=1}^{N}\left(P_{S,i} - P_{O,i}\right)^2}{N}\right]^{1/2} \tag{5}$$

$$r = \frac{\sum_{i=1}^{N} \left(P_{S,i} - \bar{P}_S\right)\left(P_{O,i} - \bar{P}_O\right)}{\sqrt{\sum_{i=1}^{N} \left(P_{S,i} - \bar{P}_S\right)^2} \sqrt{\sum_{i=1}^{N} \left(P_{O,i} - \bar{P}_O\right)^2}} \tag{6}$$

Where $P_{S,i}$ is the satellite-derived values for the i^{th} daily event, $P_{O,i}$ is the value of gauge for the i^{th} daily event, N is the total number of daily precipitation events, P_S is the average of satellite-derived values for N daily events, and P_O is the average value of gauge observations for N daily events.

Three other statistical indices, Probability of Detection (POD), False Alarm Ratio (FAR) and Critical Success Index (CSI) were also used to evaluate the precipitation detection capabilities of satellite-derived data (Wilks 2006). POD shows the proportion of the number of correct estimation of precipitation by satellite over precipitation occurrences in gauges (Equation (7)). FAR represents the ratio of cases in which precipitation is detected by satellite but not recorded in gauge (Equation (8)) and CSI demonstrates the rate of precipitation events correctly detected by the satellite (Equation (9)).

$$\mathrm{POD} = \frac{H}{H + M} \tag{7}$$

$$\mathrm{FAR} = \frac{F}{H + F} \tag{8}$$

$$\mathrm{CSI} = \frac{H}{H + M + F} \tag{9}$$

Where H is the number of cases in which observed precipitation is correctly detected by the satellite, M is the number of cases in which observed precipitation is not detected, and F is the number of cases in which precipitation is detected but not observed in gauges. POD, FAR, and CSI values range from 0.00 to 1.00, with 1 being a perfect POD and CSI and 0 being a perfect FAR (Khodadoust Siuki, Saghafian, and Moazami 2017). In the present study, a threshold of 0.50 mm day^{-1} was used to separate between precipitation and no precipitation.

Overall, IMERG and GSMaP pixels (0.10°) having at least one gauge were used. A larger number of gauges should give results that are more dependable and accurate. The methods include comparison of the rate of daily precipitation detected in two satellite-derived products with precipitation recorded in ground stations directly using nine statistical indices, as described above.

3. Results

As shown in Figure 2, the average precipitation value on the daily scale is compared for the gauges, IMERG, and GSMaP. For more clarity, the years are presented in two different charts (2016 in Figure 2(a) and 2017 in Figure 2(b)). As shown, in most cases, GSMaP remarkably overestimated the amount of precipitation in comparison with gauges. However, IMERG showed both under and overestimation.

Figure 3(a,b) illustrates the scatter plots of daily precipitation for two satellite-derived estimates versus the corresponding recorded gauge values. As shown in the figure, the

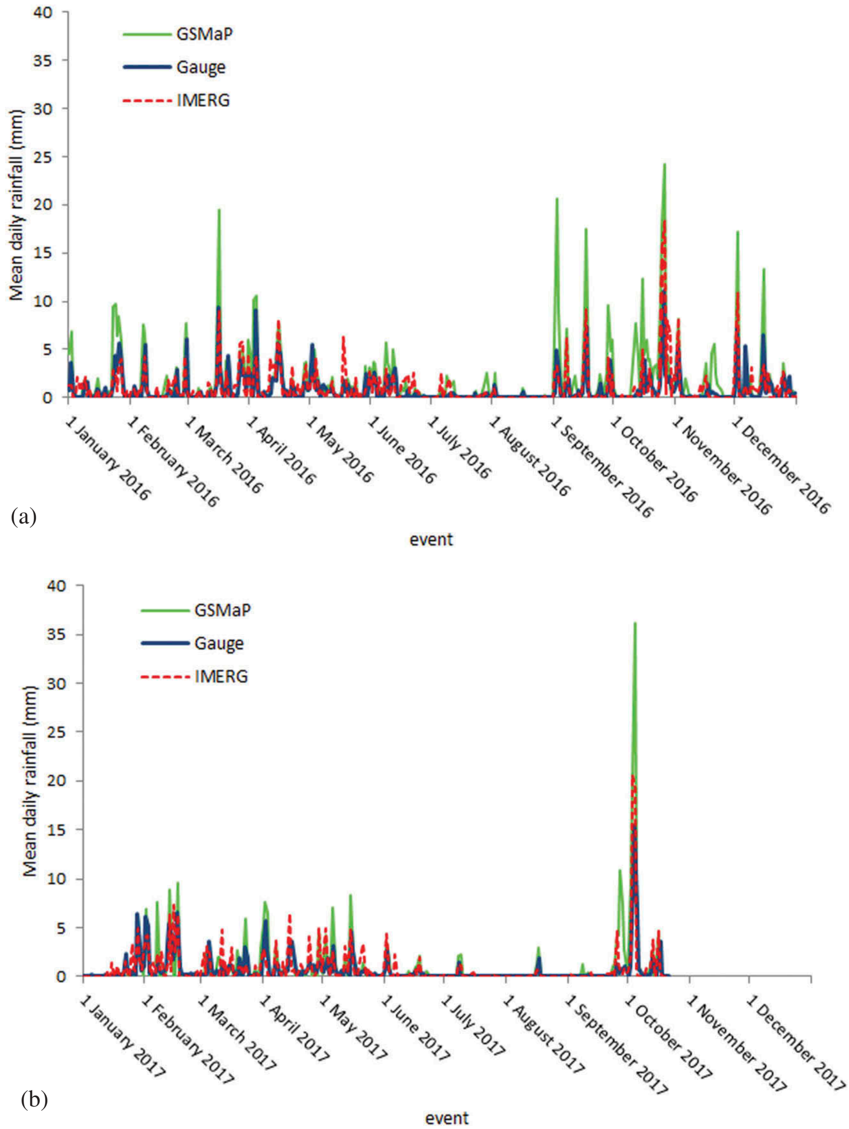

Figure 2. The average daily precipitation as measured by gauges, GSMaP and IMERG over (a) 2016 and (b) 2017.

correlation coefficient (*r*) among GSMaP estimates and gauge data is relatively higher as compared to IMERG. The results of statistical evaluation seasonally and annually are also presented in Table 1. Accordingly, the total values of B (mm day^{-1}) and B_m confirm that both GSMaP and IMERG overestimated precipitation (0.69 mm day^{-1} for B and 1.93 for B_m of GSMaP; 0.02 mm day^{-1} for B and 1.25 for B_m of IMERG). MAE and RMSE values of both IMERG and GSMaP also had remarkable differences with 0.10 and 0.83 for IMERG and 1.31 and 3.87 for GSMaP, respectively. Considering POD values, comparison of the two satellite-derived products showed that GSMaP data led to more accurate estimation for detection of precipitation in contrast to FAR values. However, CSI is equal for both of

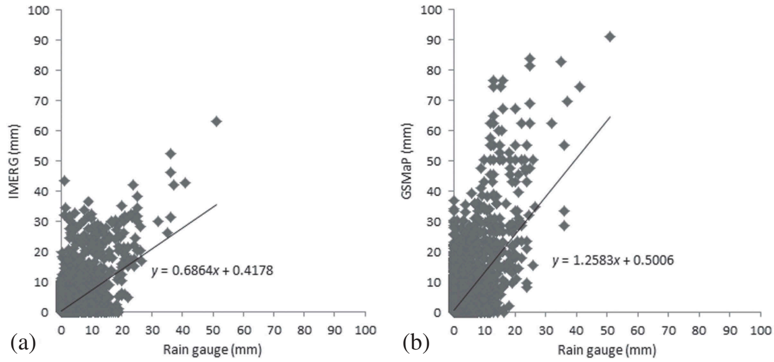

Figure 3. Scatter plots of daily values for (a) IMERG and (b) GSMaP precipitation products.

Table 1. Statistical evaluation results.

Period	Product	B (mm day^{-1})	B_m	B_r	MAE	RMSE	r	POD	FAR	CSI
Winter	IMERG	0.01	1.01	0.87	1.25	2.75	0.28	0.88	0.18	0.74
	GSMaP	0.44	1.44	44.34	1.43	4.32	0.38	0.90	0.14	0.79
Spring	IMERG	0.22	1.32	31.46	1.07	2.39	0.23	0.88	0.23	0.70
	GSMaP	0.30	2.13	43.15	0.99	2.82	0.35	0.91	0.22	0.73
Summer	IMERG	0.03	1.35	35.09	0.14	0.79	0.31	0.97	0.09	0.89
	GSMaP	0.09	4.96	109.12	0.17	0.99	0.46	0.98	0.11	0.88
Fall	IMERG	0.41	1.44	43.47	1.24	3.52	0.44	0.92	0.13	0.81
	GSMaP	1.83	2.95	195.30	2.29	5.51	0.50	0.96	0.29	0.69
Annual	IMERG	0.02	1.25	24.46	0.10	0.83	0.33	0.91	0.16	0.78
	GSMaP	0.69	1.93	92.72	1.31	3.87	0.42	0.94	0.18	0.78

them. Seasonally, there are little differences among B and B_m values of IMERG as well as GSMaP during all the seasons. However, B_r of IMERG product during winter is 0.87% and increased progressively during the following seasons. Such increased B_r also can be seen in GSMaP product after the spring. Moreover, the RMSE of both products is relatively similar and is the smallest during summer. In all the seasons, the correlation coefficient between GSMaP and gauge data is higher as compared to IMERG. With regards to POD, GSMaP showed higher ability in detecting precipitation correctly during all the seasons. Although CSI values of both products are rarely close to 1.00, it is about 0.90 during summers, which is higher than other seasons.

Figure 4(a,b) demonstrates the spatial distribution of average daily B_m in the study area where GSMaP tended to overestimate the precipitation across all (100%) selected pixels (B_m >1.00). Also, about 96% of IMERG selected pixels tended to overestimate the precipitation. According to Khodadoust Siuki, Saghafian, and Moazami (2017), if B_m lies in the 0.75–1.20 range, the satellite-derived estimates would have reasonable agreement with the gauge data. Therefore, as shown in Figure 4, GSMaP estimates were not within the mentioned range (higher than 1.28), but IMERG revealed a relatively reasonable congruence with the gauge data, as around 60% of the selected pixels accommodate the B_m range. Although there is no gauge in altitudes above 2000 m (Figure 1), the location of B_m rates of IMERG data at high altitudes particularly in the western part of the area can be concluded as a good alternative to gauges to be developed in such extremely impassable areas.

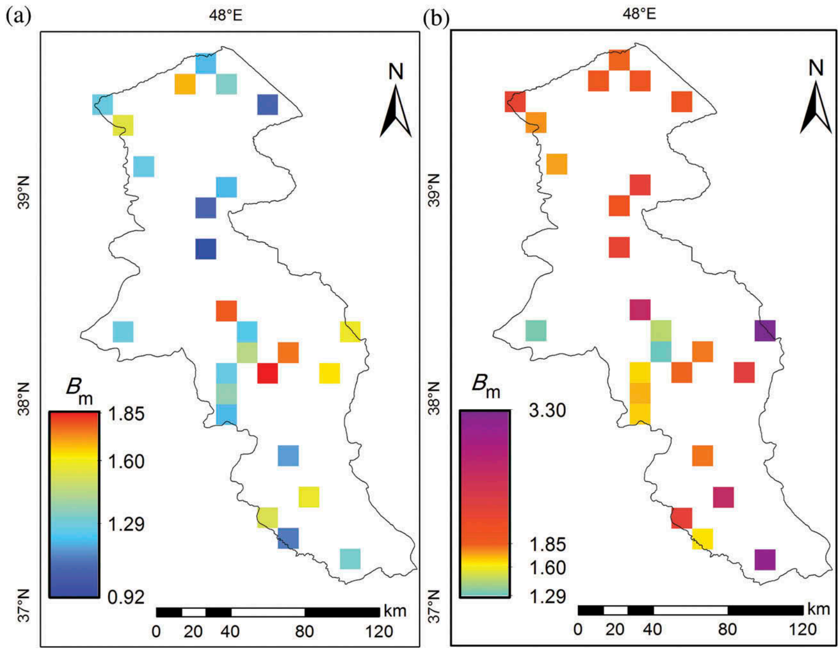

Figure 4. Spatial distribution of B_m for (a) IMERG and (b) GSMaP over the study area.

The spatial distribution of average POD values for both IMERG and GSMaP products are illustrated in Figure 5(a,b). According to the figure, both satellite-derived estimates have a relatively similar potential in detecting precipitation correctly. Although both products did not show the highest POD for the western part of the study area, they presented a reasonable performance.

Figure 6(a,b) indicates the spatial distribution of the average CSI values for IMERG and GSMaP products. As can be observed, the CSI ranges are relatively similar in both products. However, considering the pixels with the highest CSI values, both products revealed a great potential in detecting precipitation in low-altitude areas located in the north of the study area, while IMERG totally showed greater capability in detecting precipitation at high altitudes.

The main outcome of this study is displayed in Figure 7(a,b), where the average daily satellite-derived precipitation is compared with the gauge records. The values in both diagrams are in the order of highest to lowest for greater clarity. Based on this figure, GSMaP frequently overestimated precipitation, occasionally up to about 30 mm, while there is precipitation of about 15 mm in the gauge. On the other hand, a unique pattern cannot be found among IMERG estimates and gauges where IMERG frequently under and overestimated the observed precipitation. Altogether, GSMaP product indicated lower capability in detecting precipitation and presented a significant overestimation in comparison with the IMERG.

4. Discussion

In the present study, daily IMERG-Final (Version 5) and GSMaP-MVK (Version 7) precipitation products were evaluated in comparison with gauges observations in Ardabil

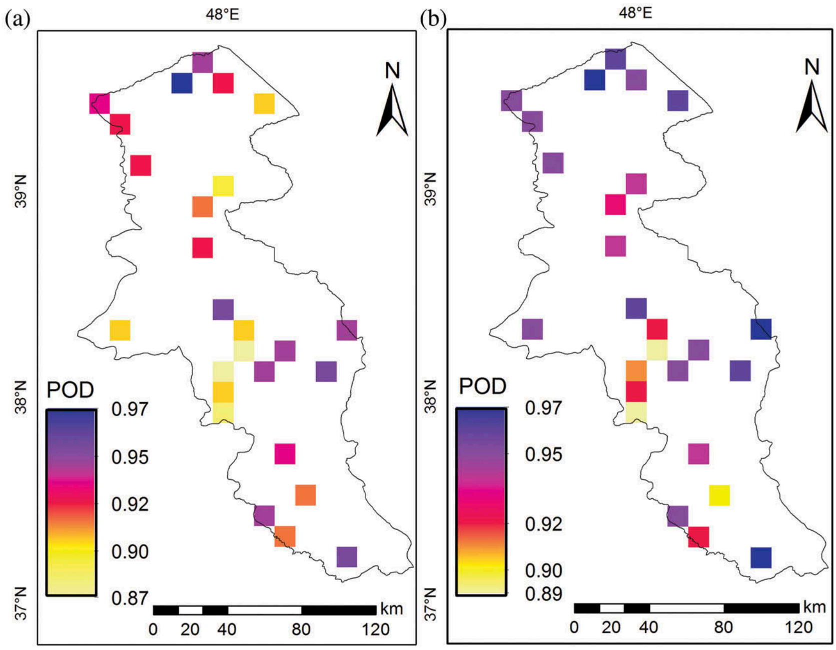

Figure 5. Spatial distribution of average daily POD for (a) IMERG and (b) GSMaP over the study area.

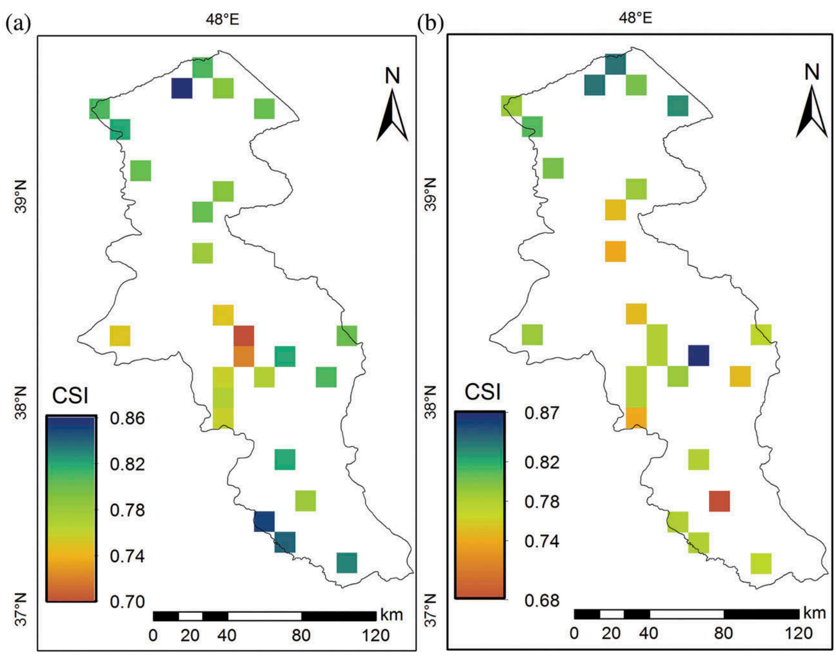

Figure 6. Spatial distribution of average daily CSI for (a) IMERG and (b) GSMaP over the study area.

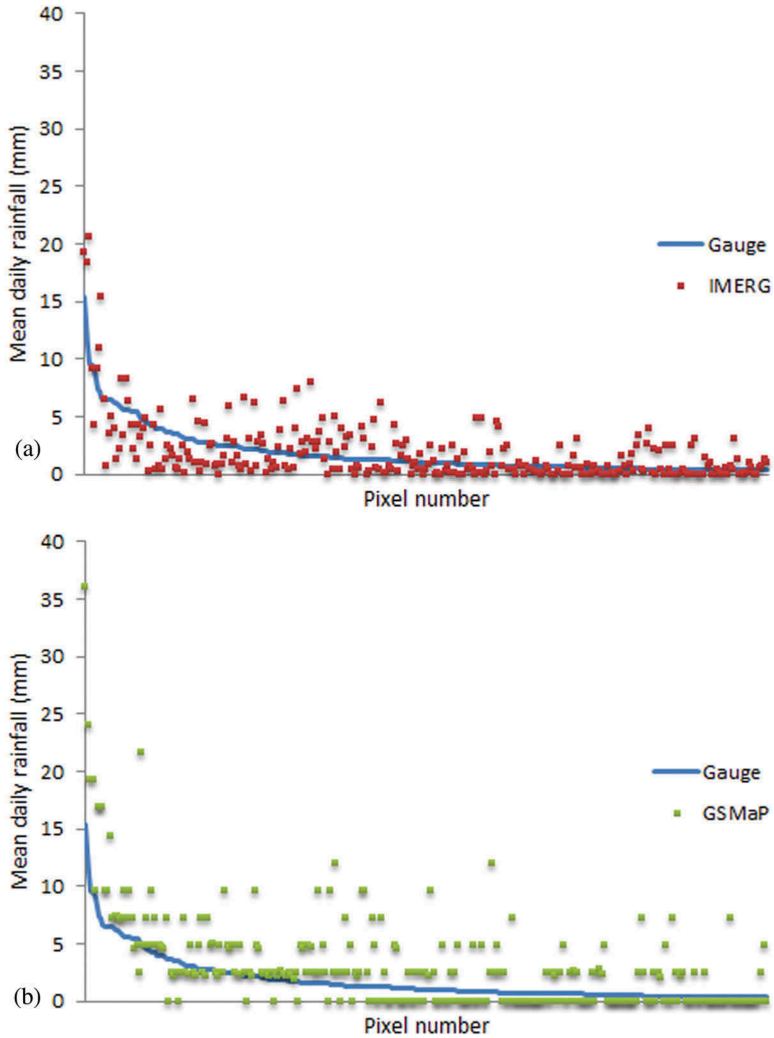

Figure 7. Comparison of average daily (a) IMERG and (b) GSMaP precipitation values with gauge data (gauge values are ordered from highest to lowest).

Province, north-west of Iran, from 1 January 2016 to 21 October 2017. Nine statistical indices were used for uncertainty evaluation, which include linear correlation coefficient, B, B_m, B_r, MAE, RMSE, POD, FAR and CSI, in both seasonal and annual scales. It was found that linear correlation among GSMaP precipitation estimates and gauge records is higher as compared to IMERG. In annual scale, evaluation of B, B_m and B_r showed that both GSMaP and IMERG products tend to overestimate precipitation. On the other hand, MAE and RMSE of both satellite-derived products have remarkable differences with higher rates for GSMaP. According to the calculated values of POD, GSMaP showed slightly higher capability than IMERG. On the seasonal scale, minor differences were observed between B and B_m values of both satellite-derived products across all the seasons. However, B_r of IMERG during winter had the minimum value, while it increased during the following seasons. Such an ascending trend in B_r has been repeated for

GSMaP after the spring. Further, both products had the least RMSE during summer. GSMaP had a better POD during all seasons. Also, both products had relatively similar CSI values, which were higher in summer in comparison with other seasons. Finally, the GSMaP product revealed less ability than the IMERG and had significant overestimation. Moreover, IMERG had some heterogeneity with gauge records but it showed the potential of use as precipitation source/input for other applications.

The results of this study showed that none of the satellite-derived products can estimate precipitation with high accuracy; however, IMERG had better agreement with the gauge records than GSMaP in the study area and can be a relatively good replacement for gauge data in regions where there are no gauges, or poor spatial and temporal coverage by gauges. The relatively good efficiency of IMERG data was underlined by other studies (Sharifi, Steinacker, and Saghafian 2016; Krishna et al. 2017; Khodadoust Siuki, Saghafian, and Moazami 2017). GSMaP substantially overestimated precipitation in this study, which is contrary to the results Ning et al. (2016), Ning et al. (2017) reported in their study area, and consistent with the findings of Prakash et al. (2016). Moreover, Islam (2018) found that IMERG and GSMaP products correctly detected the occurrence of precipitation relatively but could not estimate the accurate amount of precipitation in Bangladesh. With regards to the mentioned examples and results of other studies in different parts of the world, comparison between IMERG and GSMaP needs warrants further studies and consideration. In addition, it highlights the importance of evaluating satellite-derived products before using them under different environmental conditions. The results also indicated that using only one or two statistical indices for such evaluations can lead to a biased or invalid conclusion or interpretation (such as the correlation coefficient calculated in this study, which showed a higher correlation for GSMaP data while some other statistical indices revealed opposite results). Therefore, the use of several statistical indices helps experts to interpret their result more accurately. Forasmuch as GPM is a new tool, some challenging issues in its performance in different regions and different applications such as hydrological models will continue to remain open for future studies.

Acknowledgments

We acknowledge NASA and JAXA which provide IMERG and GSMaP data, respectively, and develop and compute their algorithms and make them accessible online. We acknowledge Ardabil Province Meteorological Organization (MO) and Ghasem Hozabrpoor (MO data officer) for providing the gauge-based data. Moreover, Mohamed Saber (Assistant Professor, Assiut University, Egypt) who helped in improving the article after the review process is appreciated.

Disclosure statement

No potential conflict of interest was reported by the authors.

References

Aonashi, K., J. Awaka, M. Hirose, T. Kozu, T. Kubota, G. Liu, S. Shige, et al. 2009. "Gsmap Passive Microwave Precipitation Retrieval Algorithm: Algorithm Description and Validation." *Journal of the Meteorological Society of Japan* 87: 119–136. doi:10.2151/jmsj.87A.119.

Aslami, F., and A. Ghorbani. 2018. “Object-Based Land Use/Land Cover Change Detection Using Landsat Imagery (A Case Study: Ardabil, Namin, and Nir Counties in Northwest Iran).” *Environmental Monitoring and Assessment* 190: 376. doi:10.1007/s10661-018-6751-y.

Bailey, T. C., and A. C. Gatrell. 1995. *Interactive Spatial Data Analysis*. London: Longman.

Bajracharya, S. R., M. S. Shrestha, and A. B. Shrestha. 2017. “Assessment of High-Resolution Satellite Rainfall Estimation Products in a Stream Flow Model for Flood Prediction in the Bagmati Basin, Nepal.” *Journal of Flood Risk Management* 10: 5–16. doi:10.1111/jfr3.12133.

Ball, J. E., and K. C. Luk. 1998. “Modeling Spatial Variability of Rainfall over a Catchment.” *Journal of Hydrological Engineering, American Society of Civil Engineers* 3: 2. doi:10.1061/(ASCE)1084-0699(1998)3:2(122).

Barrett, E. C., G. D’Souza, C. H. Power, and C. Kidd. 1988. “Toward Trispectral Satellite Rainfall Monitoring Algorithms.” In *Paper Presented at Proceedings International Symposium on Tropical Precipitation Measurements, Tokyo, Japan, NASS/NASDA*, edited by J. S. Theon and J. Fugono. Hampton, 285–292. VA: A. Depak.

Bijaber, N., D. E. Hadani, M. Saidi, M. D. Svoboda, B. D. Wardlow, C. R. Hain, C. C. Poulsen, M. Yessef, and A. Rochdi. 2018. “Developing a Remotely Sensed Drought Monitoring Indicator for Morocco.” *Geosciences* 8: 55. doi:10.3390/geosciences8020055.

Bitew, M. M., and M. Gebremicheal. 2011. “Evaluation of Satellite Rainfall Products through Hydrologic Simulation in a Fully Distributed Hydrologic Model.” *Water Resources Research* 47: 6. doi:10.1029/2010WR009917.

Chen, F., and X. Li. 2016. “Evaluation of IMERG and TRMM 3B43 Monthly Precipitation Products over Mainland China.” *Remote Sensing* 8: 6. doi:10.3390/rs8060472.

Chiu, L., D. B. Shin, and J. Kwaitkowski, 2006. “Surface Rainfall from Satellite Algorithms.” In *Earth Science Satellite Remote Sensing*, edited by J. Qu, 317–336. China: Springer Verlag and Tsinghua University Press.

Frei, C., and C. Schar. 1998. “A Precipitation Climatology of the Alps from High-Resolution Rain-Gauge Observations.” *Internationl Journal of Climatology* 18 (8): 873–900. doi:10.1002/(SICI)1097-0088(19980630)18:8%3C873::AID-JOC255%3E3.0.CO;2-9.

Griffith, D. A. 1988. *Advanced Spatial Statistics*. Dordrecht: Kluwer Academic Publishers.

GSMaP database. 2018. Accessed 2 February 2018. https://hokusai.eorc.jaxa.jp/

Guillermo, Q., G. Q. Tabios, and J. D. Salas. 1985. “A Comparative Analysis of Techniques for Spatial Interpolation of Precipitation.” *Journal of the American Water Resources Association* 21: 365–380. doi:10.1111/j.1752-1688.1985.tb00147.x.

Hermance, J. F., and H. M. Sulieman. 2018. “Adequacy of the Daily TMPA 3B42 High-Resolution Satellite Precipitation Product for Monitoring Hydrometeorological Hazards in the Southeast Sahel of Africa.” *International Journal of Remote Sensing* 39 (8): 2579–2596. doi:10.1080/01431161.2018.1430405.

Hong, Y., D. Gochis, J. T. Cheng, K. L. Hsu, and S. Sorooshian. 2007. “Evaluation of PERSIANN-CCS Rainfall Measurement Using the NAME Event Rain Gauge Network.” *Journal of Hydrometeorology*. doi:10.1175/JHM574.1.

Hossain, F., N. Katiyar, Y. Hong, and A. Wolf. 2007. “The Emerging Role of Satellite Rainfall Data in Improving the Hydropolitical Situation of Flood Monitoring in the Under-Developed Regions of the World.” *Natural Hazards* 43 (2): 199–210. doi:10.1007/s11069-006-9094-x.

Hou, A. Y., R. K. Kakar, S. Neeck, A. A. Azarbarzin, C. D. Kummerow, M. Kojima, R. Oki, K. Nakamura, and T. Iguchi. 2014. “The Global Precipitation Measurement Mission.” *American Meteorological Society* 95: 701–722. doi:10.1175/BAMS-D-13-00164.1.

Huffman, G. J., D. T. Bolvin, D. Braithwaite, K. Hsu, R. Joyce, C. Kidd, E. J. Nelkin, S. Sorooshian, J. Tan, and P. Xie. 2018. Algorithm Theoretical Basis Document (ATBD). Version 5.2. NASA Global Precipitation Measurement (GPM) Integrated Multi-satellitE Retrievals for GPM (IMERG). Greenbelt, MD 20771.

Huffman, G. J., D. T. Bolvin, D. Braithwaite, K. Hsu, R. Joyce, and P. Xie. 2014. *Algorithm Theoretical Basis Document (ATBD) Version 4.4 For the NASA Global Precipitation Measurement (GPM) Integrated Multi-satellitE Retrievals for GPM (IMERG)*. Greenbelt, MD: GPM Project. http://pmm.nasa.gov/sites/default/files/document_files/IMERG_ATBD_V4.4.pdf.

Huffman, G. J., D. T. Bolvin, and E. J. Nelkin. 2015. *Day 1 IMERG Final Run Release Notes*. Greenbelt, MD, USA: NASAGoddard Earth Sciences Data and Information Services Center.

Huffman, G. J., D. T. Bolvin, E. J. Nelkin, and D. B. Wolf. 2007. "The TRMM Multisatellite Precipitation Analysis (TMPA): Quasi-Global, Multiyear, Combined-Sensor Precipitation Estimates at Fine Scales." *Journal of Hydrometeorology* 8 (1): 38–55. doi:10.1175/JHM560.1.

IMERG database. 2018. Accessed 2 February 2018. https://disc.gsfc.nasa.gov/SSW/#keywords=imergn

Islam, M. A. 2018. "Statistical Comparison of Satellite-Retrieved Precipitation Products with Rain Gauge Observations over Bangladesh." *International Journal of Remote Sensing* 39 (9): 2906–2936. doi:10.1080/01431161.2018.1433890.

Joyce, R. J., J. E. Janowiak, P. A. Arkin, and P. Xie. 2004. "CMORPH: A Method that Produces Global Precipitation Estimates from Passive Microwave and Infrared Data at High Spatial and Temporal Resolution." *Journal of Hydrometeorology* 5 (3): 487–503. doi:10.1175/1525-7541(2004)005<0487:CAMTPG>2.0.CO;2.

Kakeh Mami, A., A. Ghorbani, F. Kayvan Behjoo, and A. Mirzaei Mosivand. 2017. "Comparison of Visual and Digital Interpretation Methods of Land Use/Cover Mapping in Ardabil Province, Iran." *Iranian Journal of Remote Sensing & GIS Techniques in Natural Resources* 8 (3): 121–134. In Persian.

Kane, M. D., G. N. Day, R. Jubach, and M. Echevers. 2000. "A Streamflow Forecasting System for the Operation of the Panama Canal." Paper presented at Watershed Management and Operations Management Conferences, Fort Collins, CO, USA, June 20–24. doi: 10.1061/40499(2000)160

Keblouti, M., L. Ouerdachi, and H. Boutaghane. 2012. "Spatial Interpolation of Annual Precipitation in Annaba- Algeria - Comparison and Evaluation of Methods." *Energy Procedia* 18: 468–475. doi:10.1016/j.egypro.2012.05.058.

Khodadoust Siuki, S., B. Saghafian, and S. Moazami. 2017. "Comprehensive Evaluation of 3-Hourly TRMM and Half-Hourly GPM-IMERG Satellite Precipitation Products." *International Journal of Remote Sensing* 38 (2): 558–571. doi:10.1080/01431161.2016.1268735.

Kim, J. P., I. W. Jung, K. W. Park, S. K. Yoon, and D. Lee. 2016. "Hydrological Utility and Uncertainty of Multi-Satellite Precipitation Products in the Mountainous Region of South Korea." *Remote Sensing* 8 (7): 608. doi:10.3390/rs8070608.

Krishna, U. V. M., S. K. Das, S. M. Deshpande, S. L. Doiphode, and G. Pandithurai. 2017. "The Assessment of Global Precipitation Measurement Estimates over the Indian Subcontinent." *Earth and Space Science*. doi: 10.1002/2017EA000285

Kubota, T., S. Shige, H. Hashizume, K. Aonashi, N. Takahashi, S. Seto, M. Hirose, et al. 2007. "Global Precipitation Map Using Satelliteborne Microwave Radiometers by the GSMaP Project: Production and Validation." *IEEE Transactions on Geoscience and Remote Sensing* 45 (7): 2259–2275. doi:10.1109/TGRS.2007.895337.

Kummerow, C. D., D. L. Randel, M. Kulie, N. Y. Wang, R. Ferraro, S. J. Munchak, and V. Petkovic. 2015. "The Evolution of the Goddard Profiling Algorithm to a Fully Parametric Scheme." *American Meteorological Society*. doi:10.1175/JTECH-D-15-0039.1.

Kurtzman, D., S. Navon, and E. Morin. 2009. "Improving Interpolation of Daily Precipitation for Hydrologic Modeling: Spatial Patterns of Preferred Interpolators." *Hydrological Processes* 23: 3281–3291. doi:10.1002/hyp.7442.

Li, X., Q. Zhang, and C. Y. Xu. 2014. "Assessing the Performance of Satellite-Based Precipitation Products and Its Dependence on Topography over Poyang Lake Basin." *Theoretical and Applied Climatology* 115: 713–729. doi:10.1007/s00704-013-0917-x.

Li, X. H., Q. Zhang, and C. Y. Xu. 2012. "Suitability of the TRMM Satellite Rainfalls in Driving a Distributed Hydrological Model for Water Balance Computations in Xinjiang Catchment, Poyang Lake Basin." *Journal of Hydrology* 426: 28–38. doi:10.1016/j.jhydrol.2012.01.013.

Luo, X., Y. Xu, and Y. Shi. 2011. "Comparison of Interpolation Methods for Spatial Precipitation under Diverse Orographic Effects." Paper presented at the 19th International Conference on Geoinformatics. Shanghai, China, June 24–26. doi: 10.1109/GeoInformatics.2011.5980666

Moazami, S., S. Golian, M. R. Kavianpour, and Y. Hong. 2013. "Comparison of PERSIANN and V7 TRMM Multi-Satellite Precipitation Analysis (TMPA) Products with Rain Gauge Data over Iran." *International Journal of Remote Sensing* 34 (22): 8156–8171. doi:10.1080/01431161.2013.833360.

Ning, S., F. Song, P. Udmale, J. Jin, B. R. Thapa, and H. Ishidaira. 2017. "Error Analysis and Evaluation of the Latest GSMap and IMERG Precipitation Products over Eastern China." *Advances in Meteorology*. doi:10.1155/2017/1803492.

Ning, S., J. Wang, J. Jin, and H. Ishidaira. 2016. "Assessment of the Latest Gpm-Era High-Resolution Satellite Precipitation Products by Comparison with Observation Gauge Data over the Chinese Mainland." *Water* 8 (11): 481. doi:10.3390/w8110481.

Okamoto, K., T. Ushio, T. Iguchi, N. Takahashi, and K. Iwanami. 2005. "The Global Satellite Mapping of Precipitation (Gsmap) Project." Paper presented at Geoscience and Remote Sensing Symposium, IGARSS '05, Seoul, South Korea, July 29. doi: 10.1109/IGARSS.2005.1526575

Prakash, S., A. K. Mitra, A. AghaKouchak, Z. Liu, H. Norouzi, and D. S. Pai. 2016. "A Preliminary Assessment of GPM-based Multi-Satellite Precipitation Estimates over A Monsoon Dominated Region." *Journal of Hydrology*. doi:10.1016/j.jhydrol.2016.01.029.

Saber, M., and K. K. Yilmaz. 2016. "Bias Correction of Satellite-Based Rainfall Estimates for Modeling Flash Floods in Semi-Arid Regions: Application to Karpuz River, Turkey." *Natural Hazards and Earth System Sciences Discussions*. doi:10.5194/nhess-2016-339.

Sawunyama, T., and D. A. Hughes. 2008. "Application of Satellite-Derived Rainfall Estimates to Extend Water Resource Simulation Modeling in South Africa." *Water SA* 34: 1–9.

Sharifi, E., R. Steinacker, and B. Saghafian. 2016. "Assessment of GPM-IMERG and Other Precipitation Products against Gauge Data under Different Topographic and Climatic Conditions in Iran: Preliminary Results." *Remote Sensing* 8: 135. doi:10.3390/rs8020135.

Skaugen, T., and J. Andersen. 2010. "Simulated Precipitation Fields with Variance-Consistent Interpolation." *Hydrological Sciences Journal* 55 (5): 676–686. doi:10.1080/02626667.2010.487976.

Skofronick-Jackson, G., W. A. Petersen, A. Y. Hou, E. F. Stocher, J. Kaye, and R. Kakar. 2013. *GPM Science Implementation Plan*. Greenbelt, MD, USA: NASA.

Su, F., Y. Hong, and D. P. Lettenmaier. 2008. "Evaluation of TRMM Multisatellite Precipitation Analysis (TMPA) and Its Utility in Hydrologic Prediction in the La Plata Basin." *Journal of Hydrometeorology* 9: 622–640. doi:10.1175/2007JHM944.1.

Tang, G., Y. Ma, D. Long, L. Zhong, and Y. Hong. 2016. "Evaluation of GPM Day-1 IMERG and TMPA Version-7 Legacy Products over Mainland China at Multiple Spatiotemporal Scales." *Journal of Hydrology* 533: 152–167. doi:10.1016/j.jhydrol.2015.12.008.

Thiessen, A. H. 1911. "Precipitation Averages for Large Areas." *Monthly Weather Review* 39: 1082–1084. doi:10.1175/1520-0493(1911)39%3C1082b:PAFLA%3E2.0.CO;2.

Ushio, T., T. Kubota, S. Shige, K. Okamoto, K. Aonashi, T. Inoue, N. Takahashi, et al. 2009. "A Kalman Filter Approach to the Global Satellite Mapping of Precipitation (Gsmap) from Combined Passive Microwave and Infrared Radiometric Data." *Journal of Meteorological Society of Japan* 87A: 137–151. doi:10.2151/jmsj.87A.137.

Watson, D. F., and G. M. Philips. 1985. "A Refinement of Inverse Distance Weighted Interpolation." *Geo-Processing* 2: 315–327.

Wilks, D. S. 2006. *Statistical Methods in the Atmospheric Sciences*. 2nd ed. Burlington, MA: Academic Press.

Xu, S., Y. Shen, and Z. Du. 2016. "Tracing the Source of the Errors in Hourly IMERG Using a Decomposition Evaluation Scheme." *Atmosphere* 7 (12): 161. doi:10.3390/atmos7120161.

Yoshinoto, S., and G. Amarnath. 2016. "Applications of Satellite-Based Rainfall Estimates in Flood Inundation Modeling—A Case Study in Mundeni Aru River Basin, Sri Lanka." *Remote Sensing* 9: 998. doi:10.3390/rs9100998.

Zeinivand, H. 2015. "Comparison of Interpolation Methods for Precipitation Fields Using the Physically Based and Spatially Distributed Model of River Runoff on the Example of the Gharesou Basin, Iran." *Russian Meteorology and Hydrology* 40 (7): 480–488. doi:10.3103/S1068373915070079.